Control of Reactivity in C−H Bond Breaking Reactions on Oxide Catalysts: Methanol Oxidation on Supported Molybdenum Oxide

S. T. Oyama,*,† R. Radhakrishnan,† M. Seman,‡ J. N. Kondo,‡ K. Domen,‡ and K. Asakura§

Department of Chemical Engineering, Virginia Tech, Blacksburg, Virginia 24061, Chemical Resources Laboratory, Tokyo Institute of Technology, Nagatsuta, Midori-ku, Yokohama 226-8503, Japan, and Catalysis Research Center, Hokkaido University, Sapporo, Hokkaido 060-0811, Japan

Received: September 9, 2002; In Final Form: November 25, 2002

Oxidation of organic substrates on metal oxide catalysts can be viewed as entailing a transfer of electrons from the organic moeity to the catalytic center, and is expected to involve the electron-accepting levels in the metal center. This investigation deals with the study of the electron-transfer processes associated with the C−H bond breaking reaction in adsorbed methoxide species in the course of methanol oxidation on supported MoO_3. It is shown that the activity of a series of catalysts duly correlates with the unoccupied density of electronic states of the parent metal oxides. The unoccupied levels are probed with near-edge X-ray absorption spectroscopy (NEXAFS). The particular system chosen for study is that of methanol oxidation on supported molybdenum oxide, a reaction in which C−H bond breaking is rate-determining. The findings of this study are in good agreement with the known facts about the reaction and allow a deeper understanding of various reported effects. For example, the positive relationships between the catalytic activity and the decreasing electronegativity of the support ion, the increasing reducibility of the dispersed molybdenum centers, and the increasing size of the molybdenum ensembles can all be explained by the increasing ease of accommodation of charge by the metal centers. The findings in this study should be of importance in understanding other C−H bond breaking reactions and multicomponent catalyst systems.

Introduction

This investigation explores the origin of the enhanced catalytic activity in the oxidation of methanol when molybdenum oxide is supported on oxide supports. The objective of our work is to present an explanation for the enhancement based on measurements of the electronic structure of the active centers by near-edge X-ray absorption fine structure spectroscopy (NEXAFS). As will be seen, the activity can be related to the density of empty electronic states available for accepting electrons in the rate-determining step of the reaction. This may be general to other systems in which a critical redox step is involved in the reaction pathway. A preliminary exposition of these ideas was presented earlier based on kinetic measurements[1] on ethanol oxidation, and the work is now expanded here for methanol oxidation.

The topic of methanol oxidation has been the subject of considerable study in the past[2−7] and intense reexamination in more recent years by the group of Wachs.[8−15] A recent in-depth study employing in situ infrared spectroscopy has revealed that on MoO_3/SiO_2 the silica support is a reservoir for reactive participating intermediates as well as inert spectators.[16] A finding of considerable interest because of its impact on multicomponent systems is the observation that supports give rise to substantial increases in activity.[1] However, despite the development of much insight on this problem,[8,10,12] a fundamental explanation of the origin of these reactivity differences has not been presented. This is important as the methanol oxidation reaction may be considered a model for reactions in which C−H bond breaking and the associated electron-transfer process is limiting.

NEXAFS has been used in the past to study electronic properties in oxides such as trends in L_2 and L_3 transition probabilities due to spin−spin coupling.[17] It has also been used to determine the local site symmetry of dispersed oxide phases from the separation in the d-orbital splitting.[18−21] This work will employ NEXAFS in a quantitative manner to obtain the trend in the density of unoccupied electronic states for a series of supported molybdenum oxide catalysts. This trend will then be related to the reactivity of the catalysts.

The methanol oxidation reaction has been studied extensively on molybdenum oxide and other related oxides and there is much that is known about the reaction. Isotopic substitution experiments on molybdenum oxide by Machiels and Sleight,[2] Holstein and Machiels,[22] and Yang and Lunsford[3] have indicated that O−H bond-breaking is equilibrated and that C−H bond-breaking is rate-determining. Consistent with this, Groff,[3] Chung and Bennett,[4] Chung et al.,[23] and Briand et al.[14] have verified by infrared spectroscopy that methoxy groups are formed on the surface of molybdenum, and Takezawa and Kobayashi,[24,25] Busca et al.,[26] Jehng et al.,[8] and Burcham and Wachs[8] on other oxides. The kinetics of the reaction on molybdenum oxide are consistent with this picture.[22,27−29]

The effect of support in methanol oxidation has also been thoroughly investigated, and there is a general concensus about the order in reactivity and the effect of loading. The first study in the molybdenum system was by Matsuoka et al.[6] who found that the order of reactivity was $ZrO_2 > TiO_2 > Al_2O_3$ and that the turnover rate increased with surface Mo coverage. No explanations were offered for these results. Subsequent studies

* Author to whom correspondence should be addressed. E-mail: oyama@vt.edu.
† Virginia Tech.
‡ Tokyo Institute of Technology.
§ Hokkaido University.

10.1021/jp0220276 CCC: $25.00
Published on Web 01/31/2003

by Kim et al.[30] and Hu and Wachs[10] confirmed the results and extended these studies. The turnover rates followed the pattern $ZrO_2 \sim TiO_2 \gg Nb_2O_5 > Al_2O_3 > SiO_2$, and increased by a factor of 2−4 as the coverage of the surface molybdenum oxide species approached monolayer coverage. This order is confirmed in our present studies.

A peculiar aspect of alcohol oxidation on MoO_3 is that the apparent activation energy, E_{app}, does not vary appreciably with support. In part, this is due to a compensation between the true activation energy for the reaction and the heat of adsorption of the methoxy precursor,[8] but the contribution of the latter is small. As will be presented in the main body of this paper, the constancy in E_{app} implies that another factor is responsible for the reactivity differences. As will be discussed, this factor resides in the preexponential of the rate constant, and can be identified with the electronic partition function.

Experimental Section

Molybdenum oxide catalysts (1 wt %) supported on ZrO_2 (Degussa, VP ZrO_2), TiO_2 (Degussa, Titanoxid P25), Al_2O_3 (Degussa, Aluminum oxid C), and SiO_2 (Cabosil L90 and Cabosil EH-5) were prepared by incipient wetness impregnation of the supports with aqueous solutions of ammonium molybdate (Aldrich, $(NH_4)_6Mo_7O_{24}\cdot 4H_2O$, > 99.99%), and subsequent drying (393 K) and calcining (773 K).

Temperature-programmed reduction (TPR) of the catalysts using continuous hydrogen flow was used to determine the onset of bulk catalyst reduction. The system used for these experiments was a flow apparatus that employed a computer-interfaced mass spectrometer (Dycor/Ametek model MA 100) for monitoring of the water production signals. The unit could also also be used for measuring oxygen uptakes of the reduced catalysts by a pulse method, as will be described shortly. All gases employed were dried with drierite/molecular sieve filters.

In the TPR measurements, the procedure employed was to begin with pretreatment of the sample (500 mg) in oxygen (Air Products, purity > 99.6%) at 773 K for 2 h to remove accumulated moisture and adventitious organic compounds. Then the flow was switched to He (Air Products, purity > 99.6%) and the sample was cooled to room temperature (RT). The reduction was carried out in 10 mol % hydrogen (Air Products, purity > 99.6%) in He from RT to 1073 K using a heating rate of 0.17 K s^{-1} (10 K/min). The mass spectrometer signal, $m/e = 18$ corresponding to H_2O, was monitored during the reduction process. The onset of bulk reduction was the temperature at which the intensity of this signal increased dramatically, and was designated as T_{red}. The temperature of the peak maximum is referred to as T_{max}.

The oxygen chemisorption studies were performed in the same apparatus used for the temperature-programmed reduction studies. The procedure involved the pretreatment of the sample (500 mg) in O_2 flow at 773 K, followed by reduction of the sample in H_2 flow for 2 h at the temperature T_{red}, determined through the TPR studies. After a brief purge in He to remove residual hydrogen and cooling to RT, the sample was dosed with 5.6 μmol pulses of high purity O_2 from a calibrated volume, while monitoring the mass spectrometer signal, $m/e = 32$ corresponding to O_2. The experiment resulted in peaks of increasing intensity which gradually reached saturation, and which were integrated to obtain the amount of oxygen chemisorbed.

The surface area measurements were carried out in a Micromeritics ASAP 2000 unit. The sample (500 mg) was loaded into a quartz reactor and degassed at 473 K in a vacuum prior to all measurements. A five-point N_2 BET analysis was used to determine the specific surface area (S_g) of each sample.

The reactivity measurements were carried out in a flow apparatus using a U-shaped quartz reactor heated in a furnace, and connected by a 10-way valve to a gas chromatograph (Shimadzu, model 14B). The valve had two sampling loops and permitted the simultaneous injection of samples into two separate columns. One was a carbosphere column attached to a thermal conductivity detector (TCD) for analysis of CO, CO_2, CH_3OH, and H_2O, and the other was a Poropak Q column attached to a flame ionization detector (FID) through a methanizer, for analysis of CH_2O. The chromatograph was calibrated through the injection of standards.

Before activity measurements, the catalysts (200 mg) were pretreated for 10 h at the highest reaction temperature (623 K, 350 °C) in a 50% O_2/He flow. The gaseous mixture used for the reaction consisted of oxygen and methanol−water vapor, diluted by helium. Flow rates were as follows: helium, 50 μmol s^{-1}; oxygen, 10 μmol s^{-1}; methanol, 3.3 μmol s^{-1}; water, 3.3 μmol s^{-1}. (Flow rates in μmol s^{-1} can be converted to cm^3 NTP min^{-1} by multiplication by 1.5.) The total flow rate (67 μmol s^{-1}, 100 cm^3/min) was in a range that resulted in conversion of methanol of approximately 5% to 20%, which was in the desirable range. The temperature for all the catalytic measurements varied between 423 and 623 K (150−350 °C). The flow rate of the methanol−water mixture was controlled by a syringe pump, which was connected through a vaporizer to the flow system. The ratio of O_2/methanol was set to a higher value than stoichiometric for the production of formaldehyde in order to keep the catalysts in an oxidized state. Blank runs using an empty reactor (no catalyst) at the conditions described above resulted in no detectable conversion of methanol up to 623 K (350 °C), demonstrating that no gas-phase reaction occurred. Also kinetic measurements on the plain supports showed very low activity up to 623 K with less than 3% of methanol conversion.

Near-edge X-ray absorption fine structure (NEXAFS) spectra for the Mo $L_{2,3}$-edges were measured at beam line BL11B of the Photon Factory in the Institute of Materials Structure Science, High Energy Accelerator Research Organization (KEK−IMSS−PF). The electron storage ring was operated at 2.5 GeV with a beam current of ~300 mA. Synchrotron radiation from the storage ring was monochromatized by a Ge(111) double crystal, and the energy resolution was about 1 eV around the Mo L_3-edge. A Cu mesh was used as the I_0 monitor and the Mo L fluorescence signal was measured by a gas flow proportional counter using Ar with 1% methane as the detector gas. The samples for the NEXAFS measurements were pretreated at 773 K for 2 h in ~30 kPa of O_2 in a recirculation system and were transferred to and sealed by glassblowing to glass cells with Kapton windows without exposure to air. The thickness of the Kapton windows was 25 μm. The NEXAFS measurements were carried out at room temperature.

Because the edge jumps in the L-edge region were small because of the low concentrations of Mo, the L-edge white lines were normalized using known amounts of $BaSO_4$ as an internal standard. The $BaSO_4$ powder (20 wt %) was physically mixed with the catalyst sample powders using a mortar and pestle, to yield a composite substance with a S/Mo ratio of 16.7. For the NEXAFS measurements these samples were treated in the same manner as the pure catalysts, and were sealed in glass cells with Kapton windows without exposure to the atmosphere. The S

TABLE 1: Summary of Catalyst Properties

catalyst	weight/mol %	T_{red} K	T_{max} K	S. A. $m^2\ g^{-1}$	O_2 uptake μmol g^{-1}	oxide dispersion %	Mo site density atoms nm^{-2}
MoO_3/SiO_2(L-90)	1/0.42	678	768	86	20	60	0.28
MoO_3/SiO_2(EH-5)	1/0.42	770	855	337	37	100	0.13
MoO_3/Al_2O_3	1/0.54	703	835	95	25	71	0.32
MoO_3/TiO_2	1/0.56	528	810	49	33	96	0.81
MoO_3/ZrO_2	1/0.85	618	886	50	31	90	0.75
SiO_2(L-90)				95			
SiO_2(EH-5)				350			
Al_2O_3				96			
TiO_2				52			
ZrO_2				50			

K-edge appears at 2472 eV, a little lower than the Mo L_3-edge at 2520 eV, and $BaSO_4$ is completely inert and stable at oxidizing conditions.

Results

Catalyst characterization results by surface area measurements, TPR, and oxygen chemisorption are summarized in Table 1. All of the supports were commercial samples prepared by flame hydrolysis of chlorides and were thus of high purity (>99.99%). Their surface areas were moderate: 95 $m^2\ g^{-1}$ for the SiO_2 (L-90), 96 $m^2\ g^{-1}$ for the Al_2O_3, 52 $m^2\ g^{-1}$ for the TiO_2, and 50 $m^2\ g^{-1}$ for the ZrO_2. Only the SiO_2 (EH-5) had a large surface area of 350 $m^2\ g^{-1}$. The surface area of the samples decreased slightly with the addition of the molybdenum oxide phase.

The temperature of reduction (T_{red}) of the samples followed the order MoO_3/TiO_2 < MoO_3/ZrO_2 < MoO_3/SiO_2(L-90) < MoO_3/Al_2O_3 < MoO_3/SiO_2(EH-5). Oxygen chemisorption uptakes indicated that the samples were well dispersed, except for the case of the low-surface-area silica-supported sample, MoO_3/SiO_2(L-90). Dispersions ranged from 70 to 100%, except for that sample which had a dispersion of 60%. Dispersions are calculated by comparing the quantity of oxygen adsorbed with the total amount of Mo in the sample assuming an O/Mo ratio of 1.0. For example, for the MoO_3/SiO_2(EH-5) sample the atomic oxygen uptake per gram of catalyst was 2×37 μmol $g^{-1} = 74$ μmol g^{-1}, while the Mo content per gram of catalyst was 1 wt % = (0.01 g MoO_3)(10^{-6} μmol mol^{-1})/(143.9 g mol^{-1}) = 70 μmol g^{-1}. The O/Mo ratio is 1.1, close to the value of 1.0 for full dispersion.

Catalytic activity is reported as turnover rates (TOR) defined as the number of methanol molecules reacted per second per surface molybdenum atoms titrated by oxygen chemisorption. The rates were calculated by summing all the products of oxidation. Mass balances closed to 100 ± 5%. The rates are displayed as Arrhenius plots in Figure 1, which also indicates the overall apparent activation energy for the catalysts. At the reaction conditions employed, all the catalysts produced only formaldehyde, CO, CO_2, and water, with the exception of alumina, which also produced methyl formate. TOR values at high conversions were out of the kinetic region and were not included. The catalytic activity measurements indicate that all catalysts behaved in a similar manner. The activation energies calculated from the data were all found within a relatively limited range of 75 and 92 kJ/mol.

Figure 2 shows NEXAFS spectra for the reference samples, Mo, MoO_3, and Na_2MoO_4 in the L_3/L_2 region. The white line areas of the samples for the L_3-edges have been shaded and the edge positions indicated. The values for the L_3-edge (2521.5 eV, 2520.7 eV, 2518.3 eV) and the L_2-edge (2625.5 eV, 2624.8 eV, 2622.0 eV) decrease in the order Na_2MoO_4 > MoO_3 > Mo foil. Since this is a qualitative comparison, the background was approximated by simple polynomial curves. It can also be seen that the white line areas are in the same order. Figure 3 shows the L_3 absorption region for the supported samples, MoO_3/TiO_2, MoO_3/Al_2O_3, and MoO_3/SiO_2(EH-5). Unfortunately the spectrum for MoO_3/ZrO_2 could not be obtained because of strong absorption by the Zr support, whose L_3- and L_2-edges at 2222 and 2307 eV, respectively, lie ahead of the Mo L_3-edge. Figures before and after background subtraction are presented. The figure before background subtraction shows that there is no measurable change in the signal for the background before and after the white line (edge jump). Figure 4 shows the L_3 region for the same samples, except that in this case the external reference, $BaSO_4$, was added to the samples. The spectra were scaled to make the signal for the $BaSO_4$ the same height. The L_3 peaks are also indicated. They appear small because of the high intensity of the $BaSO_4$ signal. Figure 5 shows an expanded

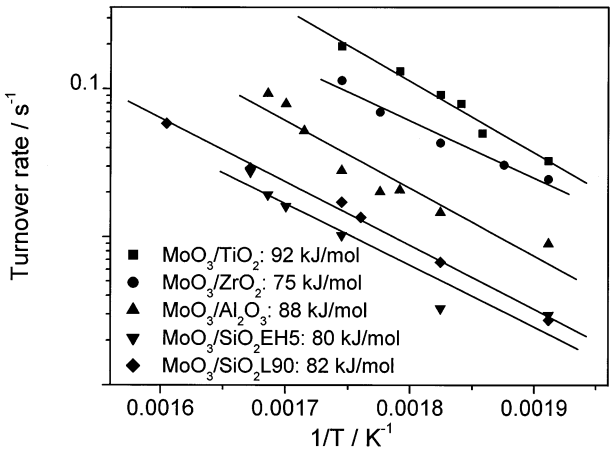

Figure 1. Arrhenius plot of turnover rates in methanol oxidation.

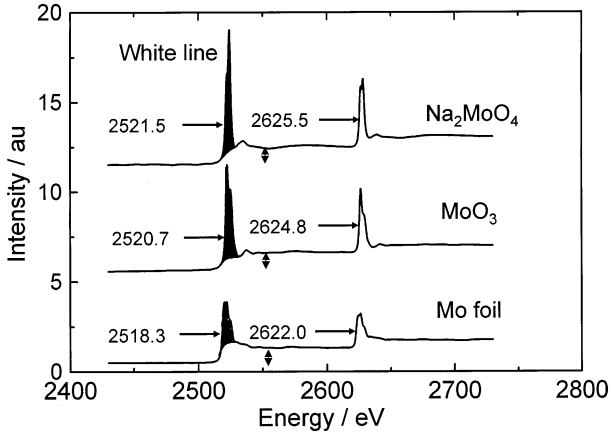

Figure 2. Effect of oxidation state on NEXAFS spectra of Mo compounds. White lines for the L_3-edge are shaded.

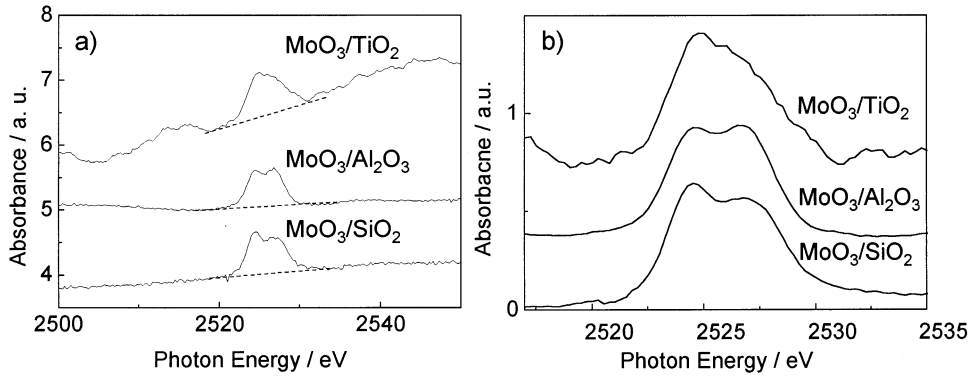

Figure 3. NEXAFS spectra of the Mo L_3-edge white line for supported molybdenum oxide catalysts: (a) before background subtraction, and (b) after background subtraction.

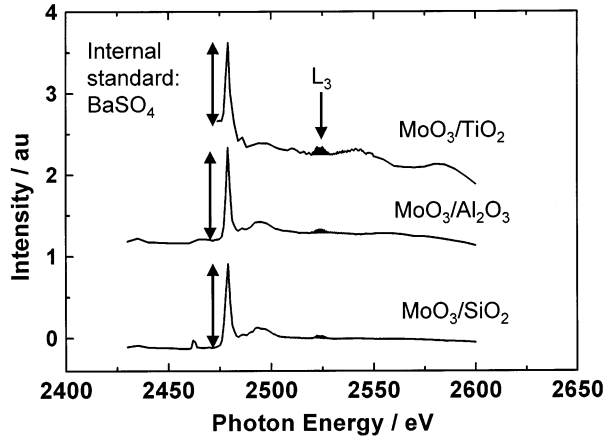

Figure 4. Effect of support on density of states for supported molybdeum oxide catalysts. The internal standard ($BaSO_4$) line at 2472 eV is indicated.

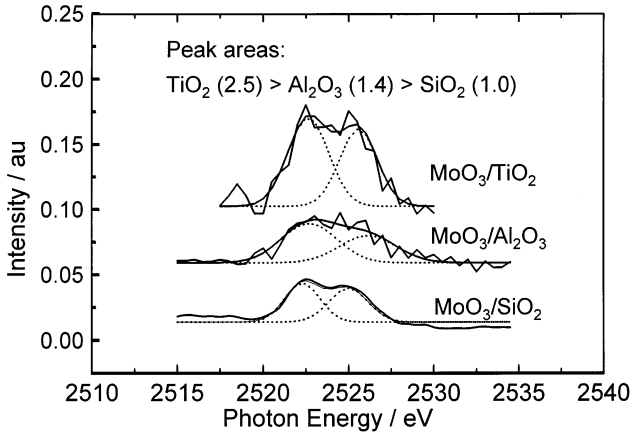

Figure 5. Relative L_3-edge white line peak areas for supported molybdenum oxide catalysts.

view of the L_3 region with the intensity normalized by the external standard $BaSO_4$. The white line areas are seen to be in the order TiO_2(2.5) > Al_2O_3(1.4) > SiO_2(1.0), with the relative intensities given in parentheses. The noise level in the MoO_3/SiO_2(EH-5) sample is the lowest because the measurement for this sample used a slightly thicker cell.

Discussion

A full study of the structure of the samples by laser Raman, NEXAFS, and EXAFS spectroscopy combined with ab initio Hartree−Fock calculations is given in a previous paper.[31] Briefly, it was found that the molybdenum species in these low loading samples were highly dispersed and had tetrahedral geometry on the Al_2O_3 and SiO_2 (EH-5) supports, and octahedral geometry on the TiO_2 support. In the low surface area SiO_2 (L-90), the molybdenum oxide was partly in the form of MoO_3 crystallites (octahedral), and partly atomically dispersed (tetrahedral). In this study the samples were further characterized by temperature-programmed reduction (TPR) and oxygen chemisorption measurements. The objective of the TPR experiments were 2-fold: first, to determine the order of reducibility of the catalysts from the positions of the onset of the reduction peaks (T_{red}); second, to determine the temperature of reduction of the catalysts prior to determination of oxygen uptakes. This was taken to be at the point of initial reduction of the samples.

From the temperature of reduction (Table 1) the ease of reducibility found was MoO_3/TiO_2 > MoO_3/ZrO_2 > MoO_3/SiO_2(L-90) > MoO_3/Al_2O_3 > MoO_3/SiO_2(EH-5). This reproduces results in the literature,[10] and its connection to reactivity will be discussed later. As just mentioned, characterization of the low-surface-area MoO_3/SiO_2(L-90) sample by laser Raman spectroscopy indicated that it had small MoO_3 crystallites while the high-surface-area MoO_3/SiO_2(EH-5) sample had atomically dispersed species. The crystallites were probably more reducible than the isolated species. Most of the reactivity work carried out in this study employed the MoO_3/SiO_2(EH-5) sample so as to avoid complications with crystalline phases and to make comparisons between well-dispersed samples.

The oxygen chemisorption measurements were carried out after reduction of the samples at the temperature (T_{red}) determined by the TPR experiments (Table 1). This permitted the use of the lowest necessary temperatures, and minimization of the possibility of compound formation with the support by overheating. The results indicate that all the samples are well dispersed (>90%), in agreement with the characterization results obtained earlier.[31] Although the Mo oxide catalysts were found to be well-dispersed (70−90%), due to the moderate surface area of the supports, the Mo species are likely to be located in close proximity. The calculated Mo site densities from the oxygen chemisorption measurements were in the range of 0.3−0.8 Mo atoms nm^{-2} (Table 1), while the monolayer density has been estimated to be 5 Mo atoms nm^{-2} by Kakuta et al.[32]

The effect of the support on the turnover rate in methanol oxidation for supported MoO_3 is shown in Figure 1. It can be seen that the apparent activation energy is close (75−92 kJ mol^{-1}) for all the samples. The order of reactivity of the supports for the MoO_3 catalysts found in this study was

$$TiO_2 > ZrO_2 > Al_2O_3 > SiO_2$$

This confirms the early results reported by Matsuoka et al.[6] and the more recent extensive studies by the group of

Wachs.[10,12,15,30] The range in activity (over 10-fold) and the order of magnitude of the turnover rates are similar to those reported by Briand et al.,[14] despite differences in the method of counting of surface sites. Our work used oxygen chemisorption, whereas the previous study employed methanol adsorption. The apparent activation energies are exactly as reported by Burcham and Wachs,[8] 84 ± 8 kJ mol^{-1}. The order of activity also tracked the results obtained on supported V_2O_5,[8,9] where an even larger range of activity was found (3 orders of magnitude).

The explanation for the effect of support builds on previous work on the system. Briefly, careful work by Hu and Wachs[10] demonstrated that the reactivity of the supported molybdenum oxide did not depend on the structure (tetrahedral or octahedral) of the Mo species. It was also indicated from kinetic[22] and isotopic substitution studies[2,3] that methanol adsorption was equilibrated, and that hydride transfer from adsorbed methoxy groups was rate-determining. Infrared studies showed that the methoxy groups leading to the main product, formaldehyde, were associated with the Mo═O functionality through addition to the double bond or adsorption on terminal oxygen vacancies.[4,23] Using the nomenclature of Holstein and Machiels,[22] where Mo* represents the catalytic center and O* an oxygen atom associated with Mo*, the known results may be expressed as follows:

$$CH_3OH + Mo^* + O^* \rightleftarrows Mo^*{-}OCH_3 + O^*{-}H \quad (1)$$

$$Mo^*{-}OCH_3 \rightarrow CH_2O + Mo^*{-}H \quad (2)$$

$$Mo^*{-}H + O^*{-}H \rightarrow H_2O + Mo^* + \square \quad (3)$$

$$O_2 + 2\square \rightleftarrows 2O^* \quad (4)$$

The reaction sequence involves the adsorption of methanol on a molybdenum center, here denoted as Mo*, likely to be a Mo═O group, to form a methoxide species. The resulting methoxy group decomposes in a rate-determining step to form formaldehyde and a hydride, here depicted to add to the Mo center, for reasons to be discussed later. The H and OH groups subsequently recombine to form water in an equilibrated step that produces oxygen vacancies, □. This last step is not critical, and may involve transfer of the hydrogen to a nearby oxygen atom to form another hydroxyl group prior to dehydration. Finally, reoxidation by molecular oxygen regenerates the oxygen sites, O*, in a step that is believed to be rapid. The overall scheme is consistent with the kinetics observed in the reaction: close to first-order in methanol, slightly negative-order in water, and slightly positive-order in oxygen. In excess oxygen, the kinetics are well described by the rate expression presented by Holstein and Machiels.[22]

$$r_{CH_2O} = k_{rds}\theta_{OCH_3} \quad (5)$$

$$\theta_{OCH_3} = \frac{K_1 K_4^{1/4}}{K_3^{1/2}} \frac{P_{CH_3OH} P_{O_2}^{1/4}}{P_{H_2O}^{1/2}} \quad (6)$$

The quantity θ_{OCH_3} is the fractional coverage of surface methoxy intermediates, k_{rds} is the rate constant for the rate-determining step (step 2), and the constants K_1, K_3, and K_4 are the equilibrium constants for steps 1, 3, and 4 in the scheme above.

Wachs and co-workers found that the activity did not correlate with the vibrational frequency of the Mo═O[10,14] and V═O[12] groups on the surface, leading them to conclude that it was the bridging oxygen moieties, Mo−O−M and V−O−M, (M = support metal) that controlled reactivity. They found that the activity correlated inversely with the Sanderson electronegativity of the metal (M), and presented several explanations for the results. Among them were that the turnover rate was determined by (a) the reducibility of the bridging Mo−O−M bonds,[10] (b) the ability of the support cation to abstract a hydride from the methoxy group,[8,15] and (c) the steady-state equilibrium adsorption of the methoxy groups on the bridging bonds.[8] These explanations are highly suggestive, but do not in themselves fully explain the reactivity differences due to the support. Sorensen and Weber have shown that the rate of methanol oxidation to formaldehyde was independent of the adjacency of V ions in heteropolytungstates substituted with 1, 2, 3, and 14 V atoms, indicating that $M_1{-}O{-}M_2$ linkages were not important.[33]

It is likely that the reactive methoxy groups are formed on the Mo═O or V═O groups by addition to the double bond or on terminal oxygen vacancies as suggested by the infrared work of Chung and Bennett.[4] It was found in supported V_2O_5[12] and MoO_3[1,8,10] catalysts that the V═O and Mo═O group Raman band intensities decreased and shifted with alcohol addition. In the latter case it was demonstrated that ethoxide groups formed on Mo═O groups were actual reactive intermediates.[34] Thus, it is likely that the role of bridging $M_1{-}O{-}M_2$ linkages is of an inductive nature providing a ligand effect on the active metal center. How this occurs will be discussed below.

Takezawa and Kobayashi[24,25] have correlated the frequencies of the C−H stretching bands of methoxy groups formed on the pure oxides of Ca, Mg, Al, Zn, Si, Ge, B, Fe, and Mo with the electronegativity of the oxide. However, examination of the infrared data reported by Burcham and Wachs[8] on supported molybdenum oxide indicates that these vibrational frequencies are unrelated to activity.

A very interesting result found in various Mo[1,8,10] and V[8,9] systems is that the apparent activation energy for alcohol oxidation is approximately constant and does not depend on support. In part this is because of cancelation of terms in the overall activation energy expression, which according to eqs 5 and 6 above is equal to

$$E_{app} = E_{rds} + \Delta H_1 + \frac{1}{4}\Delta H_4 - \frac{1}{2}\Delta H_3 \quad (7)$$

where E_{rds} is the activation energy of the rate-determining step (step 2), and the ΔH's are the heats of reaction of steps 1, 4, and 3.

Using the simplified expression, $E_{app} = E_{rds} + \Delta H_{ads}$, where ΔH_{ads} is an overall heat of adsorption, Burcham and Wachs[13] and Burcham et al.[15] found such a cancelation in the case of methanol oxidation on a variety of supported oxides. For example for vanadium oxide,[13] the correction due to ΔH_{ads} was small, and the reaction rate was dominated by the rate constant, k_{rds}, which showed a ∼22-fold increase on the oxide supports in the order Al < Ti < Zr < Ce, as opposed to K_{ads}, which showed a ∼6-fold increase.

If the same mechanism is operating with all supports and the order of magnitude of the coverage is similar in all cases, the rate given by eq 5 is seen to depend most strongly on the rate constant, k_{rds}. More specifically, since the activation energies are similar, the rate will depend on the preexponential factor, A_{rds}, of step 2. This preexponential factor is composed of contributions from the translational (q_{trans}), vibrational (q_{vib}), rotational (q_{rot}), and electronic (q_{elec}) partition functions of the activated complex. With kT/h being the universal frequency and

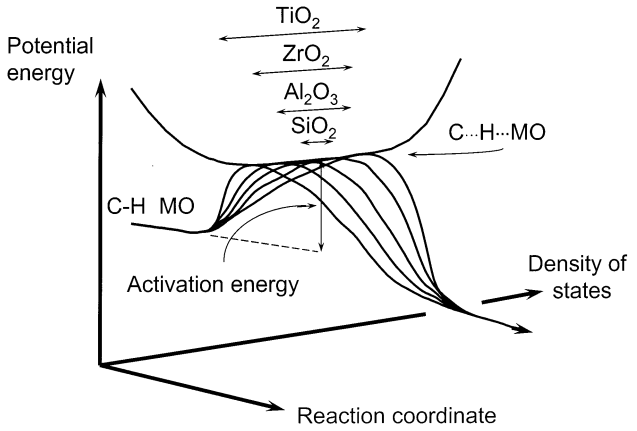

Figure 6. Energy diagram of the transition state for C−H bond breaking.

Q_{*OCH_3} the partition function of the methoxide species, the preexponential factor is given by

$$A_{rds} = \frac{kT}{h}\frac{[q_{trans}q_{vib}q_{rot}q_{elec}]^{\mp}}{Q_{*OCH_3}} \quad (8)$$

For a common methoxide intermediate, the structure and the degrees of freedom of the activated complex are expected to be of a similar order of magnitude from support to support, so that the translational, vibrational, and rotational contributions will be comparable. This leaves only the electronic partition function of the catalyst−adsorbate complex as the only likely variable to account for the difference in rates. From the order in rates in our work, it can be deduced that

$$q_{elec}(TiO_2) > q_{elec}(ZrO_2) > q_{elec}(Al_2O_3) > q_{elec}(SiO_2) \quad (9)$$

The electronic partition function is related to the density of electronic states in the catalyst complex, and the physical meaning can be understood from Figure 6. The figure shows the potential energy diagram for step 2, the rate-determining step, which is essentially a hydride transfer process from the adsorbed methoxy species to the metal center. The figure displays two coordinates, the standard reaction coordinate and an additional axis representing the density of unoccupied states of the catalyst complex for the different supports. Along the standard reaction coordinate the activation energy is depicted as constant, as found experimentally. However, along the density-of-states axis the width of the transition follows the order $TiO_2 > ZrO_2 > Al_2O_3 > SiO_2$. This order represents the number of states available to accept electrons in the hydride transfer step. When the number of states are more numerous, the number of pathways over the barrier increase, resulting in a larger preexponential factor, with the activation energy remaining unchanged.

An example of such a situation has recently been documented by Gao and Marcus[35] for a gas-phase reaction, the formation of ozone from the recombination of oxygen atoms and oxygen molecules. The authors were able to accurately predict the unconventional mass-independent reaction rates for the formation of isotopomers of ozone that had long been unexplained. For example, compared to a standard $^{16}O^{16}O^{16}O$ molecule, a molecule such as $^{17}O^{16}O^{16}O$ was found to have a larger rate constant of formation, and this was not related to mass. Gao and Marcus explained that the reason was that $^{17}O^{16}O^{16}O$ is asymmetric, so its transition state has a greater number of possible quantum states because of the greater number of vibrational and rotational couplings that can occur. Using a variational form of the statistical RRKM (Rice, Ramsperger, Kassel, Marcus) theory of bimolecular recombinations, Gao and Marcus showed that the rate constant k_{EJ} for a molecule of vibrational−rotational energy E and total angular momemtum J is

$$k_{EJ} = \frac{N_{EJ}^{\psi}}{h\rho_{EJ}} \quad (10)$$

where N_{EJ}^{ψ} is the number of quantum states accessible to the transition state, and ρ_{EJ} is the density (number per unit energy) of quantum states.

It has been assumed in the arguments above that the rate-determining step involves electron transfer to the metal center. This is consistent with the view in organic chemistry of this step being a hydride elimination.[15] According to the Born−Oppenheimer approximation, the electrons associated with the hydride are much more mobile than the proton, and would be expected to interact first with the metal. Also, the hydride elimination is consistent with oxidation being a loss of electrons by the organic moiety and a gain of electrons by the metal ion. An alternative, often cited in the literature of hydrocarbon oxidation, is proton transfer to a basic oxide center. The final resting point of the hydrogen is likely to be an oxygen atom, but in the initial stages of reaction a proton transfer would leave a negative charge on the organic species and would be a reductive process, inconsistent with oxidation. For example, in propylene, oxidation studies with different substitutents indicate that an allyl cation is the likely intermediate. The view presented here agrees with a molecular orbital study by Weber of surface methoxy C−H bond breaking by metal oxide surfaces, which indicated that hydride transfer occurred to the metal.[36] It is also consistent with ab initio calculations of hydride transfer in metal complexes by the group of Morokuma.[37]

To test the hypothesis that the rate of reaction was controlled by the density of unoccupied states available to receive the electrons transferred during the rate-determining step, measurements of the unoccupied states were undertaken using NEXAFS spectroscopy. NEXAFS has been employed in the past to measure the density of states above the Fermi level for metals[38] and compounds.[39] For the metals, a good inverse correlation was found between the area of the white line of the absorption edge and the d-band occupancy. For the compounds, the area of the white line tracked the ionic character of the bonds, I, as given by the equation of Pauling,[40] where x_A and x_B are the electronegativities of the constitutents A and B of the bonds:

$$I = 1 - \exp[-(1/4)(x_A - x_B)^2] \quad (11)$$

In the analysis of this work, the L_3-edge of molybdenum occurring at 2520 eV was chosen for the determination of the white line areas because of its high intensity. The L_3 transition is from $p_{3/2}$ core levels to unoccupied 4d levels. An illustrative set of results for reference samples consisting of Mo foil, MoO_3, and Na_2MoO_4 is shown in Figure 2. The L_3 white line areas, which correspond to transitions to unoccupied bound states, have been shaded. The spectra have been normalized so that their edge jumps, indicated by arrows, are equal. The edge jump is obtained from extrapolation of the smooth baseline before the absorption edge to a smooth region just after the absorption feature. The jump is proportional to the concentration of the absorbing element, and hence is an excellent internal standard for comparing the intensity of various resonances. In the case

of the reference samples, it can be seen that the area of the white lines increase in the order Mo < MoO_3 < Na_2MoO_4. This is the expected order from the increase in oxidation state in going from Mo to MoO_3 and Na_2MoO_4, and from the ionic character imparted to the Mo−O bonds by the electropositive Na ions (eq 10).

The L_3-edge region for the supported samples MoO_3/TiO_2, MoO_3/Al_2O_3, and MoO_3/SiO_2(EH-5) is shown in Figure 3. As mentioned earlier, the L_3-edge for Mo in MoO_3/ZrO_2 was masked by the strong adsorption of the ZrO_2 support, and could not be obtained. The spectra show distinctive features due to the white lines, but because of the low concentration (1 wt %) of molybdenum in all the samples, the edge jumps cannot be discerned. Similar results have been obtained earlier[21] in studies of the structure of the dispersed Mo centers. Without the edge jumps the white line areas cannot be quantified.

To circumvent the problem of the edge jumps, recourse was made to the addition of an external reference standard, $BaSO_4$, to the catalyst samples. The sulfur K-edge occurs at 2472 eV, so can be recorded at the same time as the Mo L_3-edge. Under oxidizing conditions $BaSO_4$ is a completely inert and noninteractive substance, and it was confirmed that little change occurred in the Mo L-edge spectral shape with its addition. The results of these measurements are shown in Figure 4. The prominent signals due to S are readily visible.

With the sensitivity properly accounted for with the $BaSO_4$ reference, it was possible to quantify the L_3-edge white line signals. The expanded region is shown in Figure 5. The relative areas (given in parentheses) are seen to fall in the order TiO_2-(2.5) > Al_2O_3(1.4) > SiO_2(1.0). This is precisely the order in the preexponential factors and electronic partition functions (eq 8) that was deduced experimentally, and supports the view that electron transfer to the oxide−support complex is limiting. The results are in agreement with the theoretical predictions of Weber.[36]

Reference has been made here to the oxide−support complex. This is to acknowledge that the metal atom is not isolated, but is in the form of a complex bound to the surface through oxygen linkages (Mo−O−M). There may be intermediate-range interactions between the Mo centers, which are not that far apart. The exact nature of the electronic structure of the complex is uncertain. Depending on the nature of the interactions the electronic levels may be highly localized or may be in the form of a substantially diffuse surface band. The support ions clearly have a major effect on the metal center. This is seen from the increase in reactivity with decreasing support electronegativity. We believe that this is due to their influence on the degree of occupancy of the electron levels. Thus, we agree with previous views that the Mo−O−M linkages are important,[8,10,12] but not so much because of the reactivity of the bridging oxygen, but because of the inductive effect on the catalytic metal center. This allows the metal to more effectively interact with the electrons during the β-hydride elimination.

It is recognized that the results presented here are limited because the characterization of the samples was carried out on the fresh catalysts. It is critical that these measurements be repeated at reaction conditions to broaden and generalize the results.

Our theory of reactivity is in accord with other observations concerning the system. For example, the observation that the catalytic activity tracks the reducibility of the metal center[10] can be traced to the relationship between reducibility and electron transfer. Since reducibility is the ability to receive electrons, the higher the density of states capable of accepting the electrons, the more reducible a substance will be. The increased activity with increasing metal oxide loading can also be understood. As the size of the ensembles grow, the electron levels form bands and the density of states increase. The conclusions of this work may have application in multicomponent systems where two metal oxides interact and in other reactions where C−H bond breaking is limiting.

Conclusions

This investigation dealt with a study of the cause for the enhancement of catalytic activity by the support in the oxidation of methanol on molybdenum oxide. It was found that the activity correlated with the density of electron accepting levels in the catalyst as probed by near-edge X-ray absorption spectroscopy (NEXAFS). It is known that C−H bond breaking in the methoxide intermediate is rate-determining in the reaction. The results suggest that electron transfer to the metal center accompanying the bond scission is the critical step.

Acknowledgment. M.S. is grateful to the Japanese government (Monbusho) for a long-term scholarship and other support. R.R. and S.T.O. thank the Director of the Division of Chemical and Thermal Systems for support through Grant CTS-9815041, and the High Energy Accelerator Research Organization at the Tsukuba Proton Factory (Grant 98G303).

References and Notes

(1) Zhang, W.; Desikan, A.; Oyama, S. T. *J. Phys. Chem.* **1995**, *99*, 14468.
(2) Machiels, C. J.; Sleight, A. W. *J. Catal.* **1982**, *76*, 238.
(3) Groff, R. P. *J. Catal.* **1984**, *86*, 215.
(4) Chung, J. S.; Bennett, C. O. *J. Catal.* **1985**, *92*, 173.
(5) Yang, T. J.; Lunsford, J. H. *J. Catal.* **1987**, *103*, 55.
(6) Louis, C.; Tatiboët, J.-M.; Che, M. *J. Catal.* **1988**, *109*, 354.
(7) Matsuoka, Y.; Niwa, M.; Murakami, Y. *J. Phys. Chem.* **1990**, *94*, 1477.
(8) Wachs, I. E.; Deo, G.; Vuurman, M. A.; Hu, H.; Kim, D. S.; Jehng, J. M. *J. Mol. Catal.* **1993**, *82*, 443.
(9) Deo, G.; Wachs, I. E. *J. Catal.* **1994**, *146*, 323.
(10) Hu, H.; Wachs, I. E. *J. Phys. Chem.* **1995**, *99*, 10911.
(11) Jehng, J.-M.; Hu, H.; Gao, X.; Wachs, I. E. *Catal. Today* **1996**, *28*, 335.
(12) Wachs, I. E.; Deo, G.; Juskelis, M. V.; Weckhuysen, B. M. In *Dynamics of Surfaces and Reaction Kinetics in Heterogeneous Catalysis*; Froment, G. F., Waugh, K. C., Eds.; Elsevier: Amsterdam, 1997; p 305.
(13) Burcham, L. J.; Wachs, I. E. *Catal. Today* **1999**, *49*, 467.
(14) Briand, L. E.; Farneth, W. E.; Wachs, I. E. *Catal. Today* **2000**, *62*, 219.
(15) Burcham, L. J.; Badlani, M.; Wachs, I. E. *J. Catal.* **2001**, *203*, 104.
(16) Seman, M.; Kondo, J.; Domen, K.; Radhakrishnan, R.; Oyama, S. T. *J. Phys. Chem. B* **2002**, *106*, 12965.
(17) Sparrow, T. G.; Williams, B. G.; Rao, C. N. R.; Thomas, J. M. *Chem. Phys. Lett.* **1984**, *108*, 547.
(18) Hedman, B.; Penner-Hahn, J. E.; Hodgson, K. O. In *EXAFS and Near-Edge Structure III*; Hodgson, K. O., Hedman, B., Penner-Hahn, J. E., Eds.; Springer-Verlag: Berlin, 1984.
(19) Bare, S. R.; Mitchell, G. E.; Maj, J. J.; Vrieland, G. E.; Gland, J. L. *J. Phys. Chem.* **1993**, *97*, 6048.
(20) Bare, S. R. *Langmuir* **1998**, *14*, 1500.
(21) Hu, H.; Wachs, I. E.; Bare, S. R. *J. Phys. Chem.* **1995**, *99*, 10897.
(22) Holstein, W.; Machiels, C. *J. Catal.* **1996**, *162*, 118.
(23) Chung, J. S.; Miranda, R.; Bennett, C. O. *J. Catal.* **1988**, *109*, 354.
(24) Takezawa, N.; Kobayashi, H. *J. Catal.* **1972**, *25*, 179.
(25) Takezawa, N.; Kobayashi, H. *J. Catal.* **1973**, *28*, 335.
(26) Busca, G.; Elmi, A.; Forzatti, P. *J. Phys. Chem.* **1987**, *91*, 5263.
(27) Chowdry, U.; Ferretti, A.; Firment, L. E.; Machiels, C. J.; Ohuchi, F.; Sleight, A. W.; Staley, R. H. *Appl. Surf. Sci.* **1984**, *19*, 360.
(28) Tatibouët, J. M.; Germain, J. E.; Volta, J. C. *J. Catal.* **1983**, *82*, 240.
(29) Machiels, C. J.; Cheng, W. H.; Chowdhry, U.; Farneth, W. E.; Hong, F.; McCarron, E. M.; Sleight, A. W. *Appl. Catal.* **1986**, *25*, 249.

(30) Kim, D. S.; Wachs, I. E.; Segawa, K. *J. Catal.* **1994**, *146*, 268.
(31) Radhakrishnan, R.; Reed, C.; Oyama, S. T.; Seman, M.; Kondo, J.; Domen, K.; Ohminami, Y.; Asakura, K. *J. Phys. Chem. B* **2001**, *105*, 8519.
(32) Kakuta, N.; Tohji, K.; Udagawa, Y. *J. Phys. Chem.* **1988**, *92*, 8583.
(33) Sorensen, C. M.; Weber, R. S. *J. Catal.* **1993**, *142*, 1.
(34) Zhang, W.; Oyama, S. T. *J. Am. Chem. Soc.* **1996**, *118*, 7173.
(35) Gao, Y. Q.; Marcus, R. A. *Science* **2001**, *293*, 259.
(36) Weber, R. S. *J. Phys. Chem.* **1994**, *98*, 2999.
(37) Koga, N.; Obara, S.; Kitaura, K.; Morokuma, K. *J. Am. Chem. Soc.* **1985**, *107*, 7109.
(38) Lytle, F. W. *J. Catal.* **1976**, *43*, 376.
(39) Lytle, F. W.; Wei, P. S. P.; Greegor, R. B.; Via, G. H.; Sinfelt, J. H. *J. Chem. Phys.* **1979**, *70*, 4849.
(40) Pauling, L. *The Nature of the Chemical Bond*, 2nd ed.; Cornell University Press: Ithaca, 1948; p 69.